PCCP

PAPER

View Article Online
View Journal | View Issue

Cite this: *Phys. Chem. Chem. Phys.*, 2017, **19**, 17360

Monitoring aggregation of a pH-responsive polymer *via* proton exchange†

Ipsita Chakraborty,[a] Ishita Mukherjee,[a] Ujjal Haldar,[a] Priyadarsi De [a] and Rangeet Bhattacharyya *[b]

Received 29th March 2017,
Accepted 12th June 2017

DOI: 10.1039/c7cp02013a

rsc.li/pccp

Understanding the changes in the macro-structure of amphiphilic pH-responsive polymers remains a relevant issue due to their potential use as drug delivery carriers. Since some of the amphiphilic polymers are known to exchange hydrogen ions with an aqueous solvent, we monitor the effective change of the surface to volume ratio of such polymer aggregates using solution-state nuclear magnetic resonance (NMR) spectroscopy. The surface to volume ratio with the help of UV-visible spectroscopy is shown to yield the average diameter of the polymer aggregates. We show that the proposed method not only satisfactorily corroborates the existing notions of how the aggregation of these polymers takes place as a function of pH, but also provides a quantitative estimate of the size of the aggregates.

I. Introduction

In recent years, pH-responsive polymers have gained importance owing to their potential use as drug delivery carriers.[1] Such polymers are also known to play important roles in the field of biomimetics and responsive plasmonics.[2] These kinds of smart polymers usually have multiple ionizable functional groups such as carboxylic acid, phosphoric acid and amines *etc.* In aqueous solutions, the presence of excess hydronium or hydroxide ions facilitates the proton exchange between the ionizable groups of the pH-responsive polymers and the solvent molecules. Aided by the exchange, such polymers in aqueous solutions may assume macro-structures depending on the nature and abundance of ionizable groups on the polymer molecules, which define the hydrophilic and hydrophobic segments. Although the hydrophobic segments form the core of the micelles, the hydrophilic ends form the coronal region. The micelles are also known to coalesce to form larger aggregates.[3] For diblock copolymers, the macro-structures are usually spherical with core–corona architecture.[3,4] The effective diameter of the micelles depends on the length of the hydrophobic part.[3]

The mechanism of formation of aggregates of micelles depends on two principle factors, namely, diffusion-limited aggregation (DLA) and repulsion between the micelles due to the accumulated surface charges.[5,6] The first factor remains dominant for the formation and growth of the aggregates,[6] whereas the second factor limits the growth process. The labile protons are exchanged between the polymer and the solvent molecules and the extent of the exchange depends on the availability of catalytic protons in the solution. The exchange renders the surface of the micelles with a partial charge which in turn prevents further aggregation through electrostatic repulsion. The competition between the two processes dictates the size and stability of the polymer suspension. Lower surface charge at higher pH results in a dominant DLA contribution which eventually leads to the formation of large-sized macro-structures which cannot be suspended and thus precipitation occurs. To monitor the structural changes of the polymer aggregates, several characterizing methods, such as fluorescence spectrometry, UV spectroscopy, dynamic light scattering (DLS), atomic force microscopy (AFM), Fourier transform infrared spectroscopy (FTIR) *etc.*, are usually used to elucidate structural changes of polymers as a function of pH.[4,7,8]

The micelles as discussed above can form aggregates through DLA. Supposing the ionizable groups exchange protons with the aqueous solvent, the ionizable groups which are deeply buried within the aggregates are not expected to undergo proton exchange and remain neutral. The surface of the small aggregates is positively charged due to the presence of excess H^+ and hinders further aggregation. At very low pH the polymer is fully soluble in water and if the concentration of the polymers is above the critical micelle concentration, then the polymers remain in a dynamic equilibrium between a free single strand form and a small micellar form.[9] Therefore, proton exchange may occur not only from the surface of the micelles (and also of the aggregates), but also from the side chains of the isolated polymer strands. Since an interface could be loosely defined considering all

[a] *Department of Chemical Sciences, Indian Institute of Science Education and Research Kolkata, Mohanpur – 741246, India. E-mail: ic12rs022@iiserkol.ac.in, ishitamukherjee08@gmail.com, haldar.ujjal10@gmail.com, p_de@iiserkol.ac.in*
[b] *Department of Physical Sciences, Indian Institute of Science Education and Research Kolkata, Mohanpur – 741246, India. E-mail: rangeet@iiserkol.ac.in*

† Electronic supplementary information (ESI) available. See DOI: 10.1039/c7cp02013a

exchange sites (surface of the aggregates as well as the isolated strands), we surmise that by monitoring proton exchange through nuclear magnetic resonance (NMR) spectroscopy one can gain insights into the interface and thereby the nature of the aggregation. There are numerous notable works on the study of interfaces using NMR spectroscopy.[10–12] However, this work uses extraction of exchange information to obtain insights into the interfacial dynamics. We show that by monitoring proton exchange by NMR spectroscopy, it is possible to gain insight into the interface of micellar aggregates and it is possible to quantitatively estimate the average size of the aggregates.

II. Protocol

To describe the protocol used for the determination of the interface of pH-responsive polymer aggregates using NMR spectroscopy, we assume that the polymer in the present context is a diblock copolymer with n repeating units having RNH_2 type side chains which form the hydrophilic part. Thus, for our system the major proton exchange mechanism which involves the solvent molecules can be represented as

$$RNH_2 + H_3O^+ \rightleftharpoons RNH_3^+ + H_2O \quad (1)$$

$$H_3O^+ + D_2O \rightleftharpoons H_2O + D_2H^+O \quad (2)$$

where R represents the group attached with the NH_2 group as a pendent of the main chain.[13,14] Since the second chemical process is not commensurate with the NMR time scale, we intend to monitor the first reaction by only observing the solvent peak.[15] The exchange was monitored using NMR spectroscopy by measuring the transverse relaxation rate of the solvent peak at various sampling frequencies, commonly referred to as a relaxation dispersion experiment. This experiment is routinely used to study the dynamics of bio-molecules.[16]

In their seminal work, Luz and Meiboom have given an expression for the variation of the transverse relaxation rate R_2 of any of the sites undergoing exchange as a function of the sampling frequency f_{cp} (inverse of the inter-π pulse distance):

$$R_2(f_{cp}) = R_{2,0} + p_A p_B \frac{\delta\omega^2}{k_{ex}}\left[1 - \frac{2f_{cp}}{k_{ex}}\tanh\left(\frac{k_{ex}}{2f_{cp}}\right)\right], \quad (3)$$

where p_A and p_B are the mole fractions of the two sites A and B, respectively, $\delta\omega$ is the frequency separation of the two sites, k_{ex} denotes the rate of chemical exchange between the sites and $R_{2,0}$ is the transverse relaxation rate of the specific site in the absence of exchange.[15] An improved form of eqn (3) was proposed by Allerhand and Gutwosky;[17] however, for our system, owing to the specific range of values of k_{ex} and f_{cp} the forms of both the equations converge to eqn (3). The transverse relaxation rate R_2 as a function of f_{cp} could be measured using the standard protocol given by Carr–Purcell–Meiboom–Gill (CPMG).[18,19] Using eqn (3), the product of the mole fractions of two sites $p_A p_B$ as well as k_{ex} could be estimated since all other parameters are either known (such as $\delta\omega = 2\pi$ 400 Hz, the difference of the chemical shifts between the amine protons and the solvent protons) or could be experimentally controlled (*e.g.* f_{cp}). The product $p_A p_B$ can also be written as

$$p_A p_B = \frac{N^{eff}_{NH_2} N_{H_2O}}{\left(N^{eff}_{NH_2} + N_{H_2O}\right)^2}, \quad (4)$$

where $N^{eff}_{NH_2}$ is the absolute number of NH_2 groups which undergo exchange, *i.e.* $N^{eff}_{NH_2}$ denotes the number of amine groups at the interface and $N^{all}_{NH_2}$ indicates the total number of amine groups in the solution.

Since for our system, $N_{H_2O} \gg N^{eff}_{NH_2}$, by rearranging the previous term we get the following:

$$p_A p_B = \left(\frac{N^{eff}_{NH_2}}{N^{all}_{NH_2}}\right)\left(\frac{N^{all}_{NH_2}}{N_{H_2O}}\right) = \alpha\beta, \quad (5)$$

where α denotes the ratio of $N^{eff}_{NH_2}$ to $N^{all}_{NH_2}$ and β denotes the ratio of $N^{all}_{NH_2}$ to N_{H_2O}. Since the amine groups buried within the aggregates do not actively take part in the exchange process, this number is expected to be smaller than the total number of amine groups in the solution $N^{all}_{NH_2}$. Since the ratio β is known *a priori*, the term α can easily be determined using eqn (5) if $p_A p_B$ is known.

Here, we have ignored the existence of isolated polymer strands in solutions and the micellar aggregation was analyzed by assuming that the aggregates possess a compact structure. Hence, the average number of such polymers that can be close-packed into a sphere of diameter d is

$$N_{agg} = \frac{\pi d^3}{6aL}, \quad (6)$$

here, a is the cross-sectional area of the hydrophobic end. So, the number of polymers on the surface of the sphere is

$$N_{surface} = \frac{\pi d^2}{a}. \quad (7)$$

Now, the total number of NH_2 *i.e.*, $N^{all}_{NH_2} = nN_{agg}$ and $N^{eff}_{NH_2} = n_1 N_{surface}$, where n_1 is the average number of NH_2 groups participating in the exchange from a single polymer molecule at the surface of a spherical aggregate. Hence, we obtain

$$d = \frac{6n_1 L\beta}{np_A p_B}. \quad (8)$$

Since all the parameters on the right-hand side of the above equation can be extracted from the NMR experiments, and if n_1 is known, then d can easily be evaluated by using eqn (8). For example, a set of CPMG experiments at various f_{cp} values can be carried out which will yield the value of $p_A p_B$. The values of n, L and β are known from the geometry of the molecule and from the concentration of the polymer solution. If n_1 is known, then the value of d can be readily estimated. To determine the value of n_1, the following strategy may be adopted: using an alternate spectroscopy the value of d can be estimated at a particular pH value for which the NMR measurements have yield $p_A p_B$. Then using eqn (8), n_1 can be estimated since the other parameters

are known. Once the estimated n_1 is available, the diameter can be found from NMR measurements at any other value of pH. UV-visible spectroscopy may provide the required alternative. The transmittance in UV-visible spectroscopy undergoes a sharp high-to-low transition when the mean wavelength of the laser is of the order of the size of the suspension. Hence, an estimate of the aggregate size is possible when the curve of UV-visible spectroscopy drops to about 50% of the maximum transmittance.

III. Experimental

To demonstrate our protocol, we have chosen an amphiphilic isoleucine-based block copolymer poly(NH_3^+-isoleucine acryloyloxyethylester)-*block*-poly(methyl methacrylate) abbreviated as (P(NH_3^+-Ile-HEA)-*b*-PMMA) and it is depicted in Fig. 1, where m and n indicate the numbers of the two types of repeating unit. As is evident from Fig. 1, the polymer contains n number of ionizable pendants with NH_2 groups dangling at the tip,[5] where n = 47 and m = 25. These amines actively take part in proton exchange with the solvent. Due to the amphiphilic nature of the block copolymer, the macro-molecules form spherical micelles, having core–corona architecture[8] with the hydrophilic NH_3^+ groups mostly at the corona.[5] Our chosen system is a cylindrical polymer of length L ($\simeq$ 20 nm) and cross sectional area a. A single spherical micelle as expected at low pH should have diameter $\simeq$ 50 nm. We note that although the labile proton of the residual carboxylic group at one end of the backbone of the polymer (Fig. 1) undergoes exchange with a water proton, its contribution in the overall exchange process is negligibly small compared with the exchange through labile amine protons as the number of amine groups present in this polymer is approximately 47 times larger than the former.

The water-soluble P(NH_3^+-Ile-HEA)-*b*-PMMA block copolymer was synthesized according to the procedure reported earlier.[5,20] The detailed synthesis process and proton NMR characterization of the copolymer and its corresponding homopolymer are given in the ESI.† Other required characterizations done by Advanced Polymer Chromatography (APC) and ^{1}H NMR are given in Table 1.

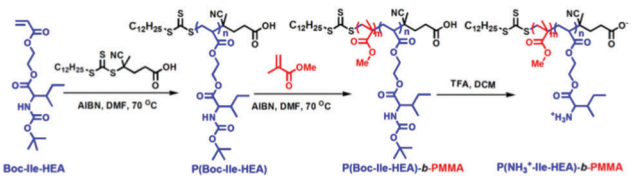

Fig. 1 A schematic representation of RAFT mediated block co-polymerization of Boc-Ileu-HEA and MMA monomers, followed by deprotection of the Boc group to enable proton exchange between the hydronium and labile amine groups.

Reversible addition-fragmentation chain transfer (RAFT) mediated block co-polymerization of *tert*-butyl carbamate(Boc)-isoleucine acryloyloxyethyl ester (Boc-Ile-HEA) and methyl methacrylate (MMA) monomers, followed by the deprotection of the Boc group, is schematically represented in Fig. 1 (for details please refer to the ESI†). 32 mg of the freshly prepared and purified compound was dissolved in the mixture of 4 mL HPLC water and 4 mL D_2O to make an approximately 0.03 μM solution. The pH was monitored by pH-meter and was adjusted using 0.1 N HCl and 0.1 N NaOH. The accuracy of reported pH was 0.1 and seven different solutions of pH 3.0, 4.0, 5.0, 5.5, 6.0, 6.5, and 7.0 were prepared. All the experiments were performed within 3 to 4 hours of preparing the solution. A similar set of pH solutions was prepared taking only a 1 : 1 D_2O and H_2O mixture, without any polymer.

All the NMR experiments were performed at room temperature using an 11.78 T Bruker Avance III spectrometer with an operating proton Larmor frequency at 500.23 MHz. The R_2 values were estimated using the standard CPMG pulse sequence for ten different sampling frequencies uniformly selected between 80 Hz and 20 kHz (corresponding to CPMG delay of 100 ms to 50 μs). All the CPMG experiments were performed with 15 s recycle delay, which ensures complete relaxation of the water protons. The power used for all the pulses (excitation and refocusing) was 17.8 kHz.

Fig. 2 shows the R_2 *versus* f_{cp} plots for the aqueous solutions with (circles) and without (squares) the polymer suspension, where the pH values of both the solutions were 3.0. The data were individually fit with eqn (3) and the solid and dashed lines represent the fit for the solutions with and without polymer respectively.

The UV visible study was performed on a Perkin-Elmer Lambda 35 UV-visible spectro-photometer for the aqueous sample solutions (4 mg mL^{-1}) at ten different pH values ranging from 3.0 to 10.0. The samples were placed in a quartz cuvette to measure the transmittance, where the scanning range of incident monochromatic light was 400 nm to 600 nm and the transmittance at each value of pH was recorded.

The zeta potential of the aqueous solution of polymer at seven different pH values was measured at room temperature (25°) using a dynamic light scattering (DLS) (Zetasizer Nano ZS, Malvern Instrument Ltd, UK) instrument equipped with a He–Ne laser beam.

IV. Results and discussion

From the results, obtained from the CPMG experiments, R_2 has been extracted for all f_{cp} using the mono exponential decay fit. From the R_2 *versus* f_{cp} data fit, $p_A p_B$ and k_{ex} were extracted

Table 1 Copolymer molecular characteristics

Polymer	Conversion[a] (%)	M_n, APC[b] (g mol^{-1})	PDI[c] (Đ)	$M_{n,NMR}$[d]	$M_{n,theo}$[e]	^{1}H NMR composition[f] (mol%)
P(Boc-Ile-HEA)$_{47}$-*b*-PMMA$_{25}$	90	17 800	1.15	18 300	16900	Boc-Ile-HEA : MMA [47 : 25]

[a] Calculated gravimetrically. [b] Measured by APC. [c] Measured by APC. [d] Determined by ^{1}H NMR study. [e] $M_{n,theo}$ = (([monomer]/[CTA] × molecular weight (M_W) of monomer × conv.) + (M_W of CTA)). [f] Repeating unit composition of Boc-Ile-HEA and MMA, as determined by ^{1}H NMR.

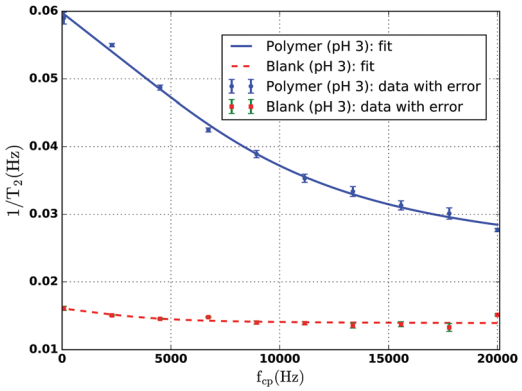

Fig. 2 Plots of R_2 *versus* f_{cp} data with error bars for the solution with polymer (blue circles) and the blank solution (red squares) at pH 3.0. The corresponding fits with eqn (3) are indicated by the continuous and dashed lines respectively.

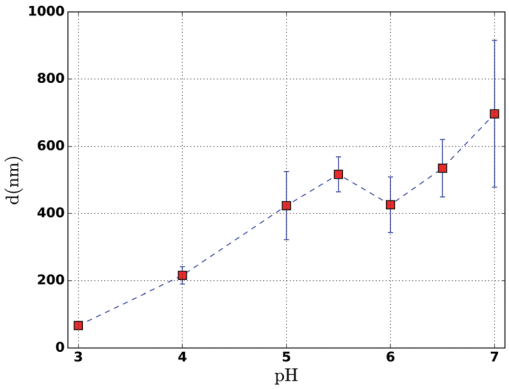

Fig. 4 The calculated diameter (nm) of the aggregates using NMR as a function of pH as determined from eqn (8). The lines are eye-guides to highlight the trends of the relevant part of the experimental data. The error was estimated from eqn (8) and using partial error analysis from the individual contribution of the parameter.

using eqn (3). It is clearly evident from Fig. 2 that having a polymer suspension has a pronounced effect on the R_2 values as a function of sampling frequency whereas the blank solution without polymer suspension does not have any pronounced effect on the same. Hence, our proposition is that only the first reaction, the chemical eqn (1), remains validated for this study.

From the UV-visible study, we have estimated the value of n_1 in the following way: we assume that at the pH value when the transmittance drops below 50% of the starting point, the average diameter of the aggregates is of the order of mean λ ($\approx$ 500 nm) used for measuring transmittance. Therefore, substituting the value of 500 nm as diameter, eqn (8) yields $n_1 \approx 26$, *i.e.* about 26 amine groups out of 47, from each polymer strand from the surface of the aggregates take part in the exchange process.

The knee-like regime in the plot of transmittance (%) *versus* pH in Fig. 3 indicates partial transmission from pH 5.5 to 6.5 which appears because of the large size distributions of the existing macro structures. The percentage of transmittance of the incident light (scanning range 400 nm to 600 nm) *versus* pH clearly shows that at lower pH, from 3 to 5, the average size of the macro structures is less than 400 nm, from pH 5 to 6.5 it lies in between 400 nm and 600 nm and after that further increase in pH shows a rapid and large amount of loss of transmittance (less than 50%), which indicates that the average size of the particles is bigger than 600 nm. The information about particle size, obtained from the UV-visible study, qualitatively matches with the data, extracted from NMR experiments (Fig. 3 and 4).

It is observed from Fig. 5 that the increase in the calculated diameter (d) is nearly linear with the increase of pH. At pH 5.5 the value of d drops suddenly and starts rising again from pH 6. A possible explanation of this behaviour could be that at very low pH (about 3) a significant number of single polymer strands remain in dynamic equilibrium with single micelles in the aqueous solution.[8] As the pH increases slowly, the isolated micelles keep aggregating and result in larger sized macro-structure. Hence, it is obvious that there would be a loss of interface and the increasing trend in d between pH 3 to 5.5 supports our claim. Once the isolated single strands are

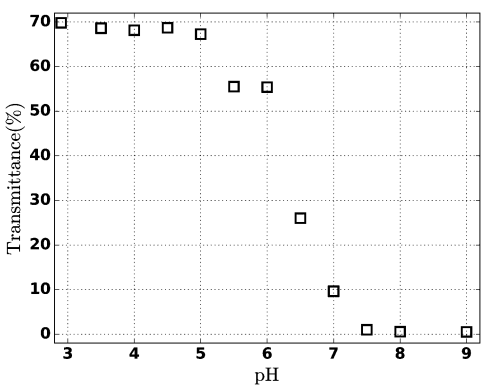

Fig. 3 The percentage of transmittance (%) as a function of pH as determined from the UV-vis study.

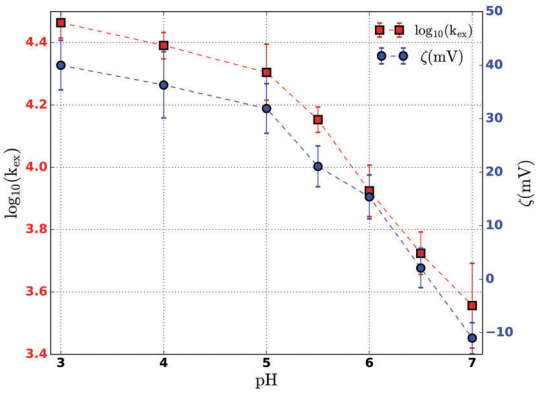

Fig. 5 (i) The k_{ex}, determined using NMR and (ii) the zeta potential of the aggregates obtained from the DLS study, as a function of pH. k_{ex} was determined from eqn (3). The squares represent the logarithm (to the base 10) of exchange rate k_{ex} (with the y axis on the left) *vs.* pH, and the circles represent the zeta potential (ζ) in mV (with the y axis on the right) *versus* pH. The lines are eye-guides to highlight the trends of the relevant part of the experimental data.

depleted, a sudden decrease in diameter can happen if the micellar aggregates start forming more compact super-aggregates. Since the electrokinetic potential also goes below 30 mV at this point, micellar aggregation is possible. It is possible that at around pH 5.5 the aggregates have a long rod- or chain-like structure (confirmed by SEM, shown in Fig. S4 in the ESI†). The smoothening of the surface would lead to a decrease in the effective diameter. Beyond pH 6, we observe an increasing trend in d which can be attributed to further micellar aggregation. The results of DLS on the polymer suspension at a similar set of pH values support the increasing trend of the aggregate size (see Fig. S3, ESI†).

To further corroborate our speculation, the images of the drop casting of the very diluted sample solutions prepared at four different pH values were captured using a Scanning Electron Microscope (SEM). The SEM images qualitatively confirm our result as shown in Fig. S4 in the ESI.†

The proton exchange rate is assumed to depend solely on the availability of the labile protons at the interface, when the temperature is kept fixed. However, it is observed from the k_{ex} data (circles with red short-dashed trend lines) in Fig. 5 that within the range of pH 3 to pH 5, the exchange rate k_{ex} suffers from a slow decay whereas beyond pH 5 the rate drops at a faster rate.

It is expected that the proton exchange between the bulk solution and the surface of the aggregates will have strong dependence on the repulsive surface charge of the aggregates. Since the electrokinetic potential is a well-defined measure of the surface charge accumulation of the suspension, it is contemplated that the proton exchange rate and the electrokinetic potential should be correlated.[21]

Fig. 5 shows the changes of the proton exchange rates k_{ex} and the electrokinetic potential as a function of pH. The plot shows that below pH 5, the electrokinetic potential is more than 30 mV and thereby suggests a stable micellar structure and less aggregation. Beyond pH 5, the electrokinetic potential drops below 30 mV and micellar aggregation starts. This assertion is also supported by UV-visible spectroscopy described earlier and the results from SEM and DLS (ESI†). It is clearly evident from Fig. 5 that there exists a strong correlation between the proton exchange and eletrokinetic potential.

The protons – being positively charged – would experience the eletrokinetic potential as an energy barrier in the process of hopping of the proton from the solvent site to a neighbouring site on the surface of the aggregates. Therefore, the behaviour that k_{ex} is proportional to ζ is counter-intuitive. However, for such aggregates, the electric double layer (EDL) is formed and as a result the potential drops at a faster rate outside the surface. This allows a closure approach of the protons to the surface of the aggregates. As a result, this negatively charged diffusive layer is expected to facilitate the exchange process. The role of EDL or rather the negatively charged layer favouring the exchange process is clearly confirmed from Fig. 5, which shows that at higher surface charge the exchange rate is also high and *vice versa*. A detailed investigation of the exact microscopic processes involved remains an open area of research for this class of polymer aggregates. Also, as is observed in the case of k_{ex}, the zeta potential also undergoes a slow change in the pH range 3–5 and drops at a faster rate in the pH range 5–7. The electrokinetic potential depends on the surface charge of the aggregates which would be a function of the total effective surface area of the aggregates present in the solution. With the increase in pH the total effective surface area is expected to decrease with two different rates. Up to some moderate pH (4–5), as long as a significant number of single strand polymers and very small sized micelles exist in the solution, the effective surface area would drop slowly and beyond pH 5 it should fall rapidly as it starts to form a larger spherical structure.

In view of the preceding discussion, we venture to suggest that up to about pH 5 a significant number of single strands of polymer are present in the solution which owing to their small size can exchange protons with greater ease with the aqueous solvent and hence k_{ex} does not experience a sharp drop. In contrast, once the single strands are depleted (all are attached to the smaller aggregates), the exchange rate drops sharply indicating that the macro-structures are in the process of forming bigger super-structures, *i.e.* as the pH increases the micelles join one another to form super-structures which may no longer remain suspended. Consequently, Fig. 5 shows a nice correlation between these two phenomena.

V. Summary and conclusions

By using the standard CPMG experiments available with all NMR spectrometers, we show that the calculated values of the exchange rate and the interface (more strictly, surface to volume ratio) completely corroborate known behaviour of at least a class of pH-responsive polymers. Although DLS and other scattering methods show the shape and size of the aggregates, such methods may not be suitable to estimate the average diameter (or interface) of the polymer aggregates. UV-visible spectroscopy yields the transmittance of the suspension, which, unless undergoing a significant change in intensity, does not provide an estimate of the average size. The DLS studies readily provide intensity-size distribution; however, number-size distribution which is more informative relies on accurate knowledge of the refractive index of the suspended particles. Also, DLS usually yields the hydrodynamic radius which is different from the actual size of the aggregates. In contrast, our proposed method, being reliant on the exchange from the true surface, yields a more accurate estimation of the average size of the aggregates and hence of the radius of gyration. Therefore, monitoring proton exchange by NMR spectroscopy yields insights into the overall surface to volume ratio (approximately the measure of the interface) and in conjunction with UV-visible spectroscopy directly yields an estimate of the average diameter of the aggregates. Therefore, the proposed method clearly enjoys superiority over light scattering methods for the extraction of the average aggregate diameter.

Acknowledgements

The authors gratefully acknowledge IISER Kolkata for providing the necessary funding and the NMR facility where the work has been carried out. We thank Dr. Rumi De for her valuable

suggestions and Binoy Maiti and Mridula Nandi for the assistance with the scattering experiments. I. C. thanks Council of Scientific and Industrial Research (CSIR), for a research scholarship.

References

1 D. Schmaljohann, *Adv. Drug Delivery Rev.*, 2006, **58**, 1655–1670.
2 H. Zhang, Y. Tian, J. Hou, X. Hou, G. Hou, R. Ou, H. Wang and L. Jiang, *ACS Nano*, 2015, **9**, 12264–12273.
3 D. Lombardo, M. A. Kiselev, S. Magazú and P. Calandra, *Adv. Condens. Matter Phys.*, 2015, **151683**, 1–22.
4 B. P. Bastakoti, S. H. Liao, M. Inoue, S. I. Yusa, M. Imura, K. Nakashima, K. C.-W. Wu and Y. Yamauchi, *Sci. Technol. Adv. Mater.*, 2013, **14**, 044402.
5 K. Bauri, S. Ghosh Roy, S. Pant and P. De, *Langmuir*, 2013, **29**, 2764–2774.
6 T. A. Witten, Jr. and L. M. Sander, *Phys. Rev. Lett.*, 1981, **47**, 1400–1403.
7 J. Humpolíčková, M. Štěpánek, K. Procházk and M. Hof, *J. Phys. Chem. A*, 2005, **109**, 10803–10812.
8 M. Karayianni and S. Pispas, *Self Assembly of Amphiphilic Block Copolymer in Selective Solvents*, Springer International Publishing Switzerland, 2016, vol. 16, pp. 27–63.
9 M. Doi, *Soft Matter Physics*, Oxford University Press, 2013.
10 H. Takahashi, T. Nakanishi, K. Kami, Y. Arata and I. Shimada, *Nat. Struct. Biol.*, 2000, **7**, 220–223.
11 R. Bhattacharyya, K. Baris, H. Chen, A. S. Best, A. F. Hollenkamp and C. P. Grey, *Nat. Mater.*, 2010, **9**, 504–510.
12 F. Berti, P. Costantino, M. Fragai and C. Luchinat, *Biophys. J.*, 2004, **86**, 3–9.
13 E. Grunwald, A. Loewenstein and S. Meiboom, *J. Chem. Phys.*, 1957, **27**, 630–640.
14 S. W. Englander, N. W. Downer and H. Teitelbaum, *Biophys. J.*, 2009, **96**, 2045–2054.
15 Z. Luzand and S. Meiboom, *J. Chem. Phys.*, 1963, **39**, 8972–8979.
16 P. Neudecker, P. Lundström and L. E. Kay, *Biophys. J.*, 2009, **96**, 2045–2057.
17 A. Allerhand and H. S. Gutowsky, *J. Chem. Phys.*, 1965, **42**, 1587–1599.
18 H. Y. Carr and E. M. Purcell, *Phys. Rev.*, 1954, **94**, 630–638.
19 S. Meiboom and D. Gill, *Rev. Sci. Instrum.*, 1958, **29**, 688–691.
20 U. Haldar, M. Nandi, B. Ruidas and P. De, *Eur. Polym. J.*, 2015, **67**, 274–283.
21 J. B. Matthew and F. M. Richards, *J. Biol. Chem.*, 1983, **258**, 3033–3044.